SCALAR PULSE WIDTH MODULATION STRATEGIES FOR MATRIX CONVERTERS

A. G. H. Accioly, V. N. Lima, F. Bradaschia, F. A. S. Neves, M. C. Cavalcanti, A. Samuel Neto
Departamento de Engenharia Elétrica e Sistemas de Potência, UFPE. Recife - PE - Brasil
Emails: andre_ guga@yahoo.com.br, vnuneslima@gmail.com, fabricionet@yahoo.com.br,
fneves@ufpe.br, marcelo.cavalcanti@ufpe.br, asneto01@yahoo.com.br

***Abstract*— This paper describes three different scalar pulse width modulation (*PWM*) techniques for matrix converters to be compared to two other scalar techniques proposed here. Before exposing all the techniques, a mathematical review of the matrix converters is done to aid the comprehension of this converter. These new techniques use, for synthesizing an output reference voltage, only two input voltages in each switching period. As consequence, the losses of the switching process are expected to be lower than the losses of the other techniques. All techniques presented, but one, have unity displacement factor (*DF*). To verify the characteristics of these new methods, some simulation results are presented and compared with some simulation results presented by the other methods.**

***Keywords* - AC-AC Power Conversion, Frequency Converters, Pulse Width Modulation, Simulation.**

I. INTRODUCTION

The first study about matrix converters was presented in 1976 by *Gyugyi* and *Pelly* [1]. Later, in 1980, *Venturini* and *Alesina* in [2] and [3] introduced the term "Matrix Converter" and presented the first algorithm capable of synthesizing output sinusoidal reference voltage with any frequency, from a balanced three-phase grid located at the converter input terminals (Fig. 1).

Differently from usual frequency converters (*AC-DC-AC*), the matrix converter is a direct frequency converter. In this type of converter, the input is considered as a voltage source and, because the inductive nature of the load, the output terminals are considered as current sources. Output voltages, with target amplitude and frequency, are produced through the sequential switching of the input voltages (in other words, the output voltages are made from "pieces" of the input voltages). The currents flowing to the input terminals are obtained through the "segments" of the output currents.

Due to the direct frequency conversion, the matrix converter does not need bulky storage devices used in the traditional converters. Thus, reactive elements are only necessary to compose the input and the output filters. Because of its inductive nature, the load can often be used as an output filter for the high frequency components.

Because of the absence of the dc link, it should be observed that, in an ideal conversion, the instantaneous value of the input power is always equal to the instantaneous value of the output power.

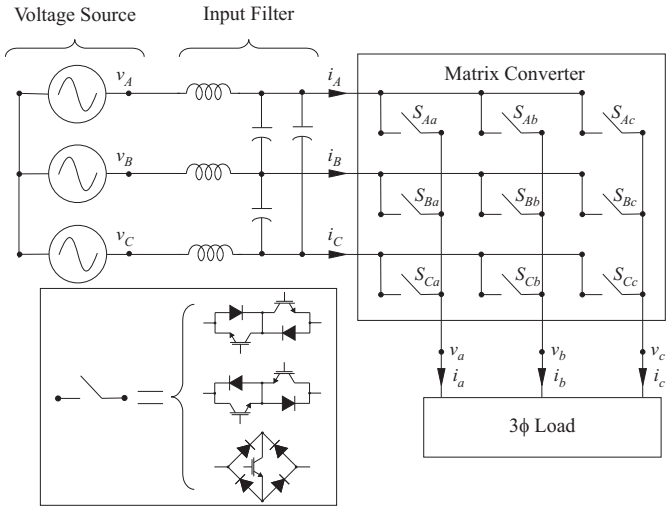

Fig. 1. Simplified circuit of a 3×3 matrix converter.

The switches shown in Fig. 1 are bidirectional switches. They permit the energy flows from the grid (input terminals) to the load and from the load to the grid. One of the major problems of the matrix converter is related to the lack of high power bidirectional semiconductors devices. In this way, it is necessary to use an arrangement with available devices - for example diodes and *IGBT*s (Insulated Gate Bipolar Transistor).

The detail in Fig. 1 presents some possibilities to build the bidirectional switches. One of them consists of an *IGBT* at the center of a single-phase diode bridge arrangement. The main advantages are that both current directions are carried by the same switch device and only one gate driver is required per commutation cell. As disadvantages of this structure, the conduction losses are relatively high since there are three devices in each conduction path and the direction of current cannot be controlled [4].

The other two arrangements are known as common emitter and common collector back-to-back switch and they are two variations of the same principle. These bidirectional switches possibilities consist of two diodes and two *IGBT*s connected in anti-parallel. The diodes are included to provide the reverse blocking capability. Comparing with the previous example, these structures have several advantages. It is possible to control the direction of the current and the conduction losses are reduced since only two devices carry the current at any one time [4].

Manuscript received on June 30, 2006. First revision on August 14, 2006. Second revision on October 25, 2006. Recommended by the Editor Richard M. Stephan.

A compact matrix converter would only be possible if a module containing all 9 bidirectional switches were built. Observing the continuous growth of the interest at this kind of frequency converters, *Eupec*, in cooperation with *Siemens*, developed the first power integrated module, called *EconoMAC*. In Fig. 2 is shown this module for a $7.5kW$ matrix converter [5] and [6]. In this module, the common collector back-to-back switch topology is employed, resulting in only 6 connections which need to be fed correctly to activate each gate [6]. This arrangement leads to a very compact converter with the potential for substantial improvements in efficiency.

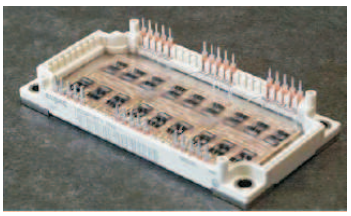

Fig. 2. The *Eupec EconoMAC* matrix module.

As the output voltages are synthesized from the input voltages, because of the absence of storage devices, there is an intrinsic limit in the output voltage amplitude. If the output reference phase voltages are sinusoidal, three-phase and balanced, this intrinsic limit is 50% of the input phase voltage amplitude, as shown in Fig. 3.

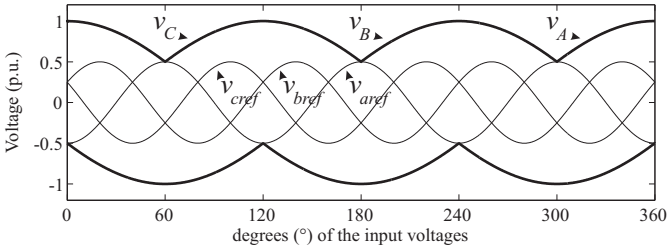

Fig. 3. Maximum voltage ratio of 50%.

In Fig. 3, it is observed that there are regions, involved by the input voltages, that are not used by the output voltages. *Maytum*, in 1983 [7], as well as *Alesina* and *Venturini*, in 1988 [8], demonstrated that, using these regions, the output voltage limit can be increased to 87% of the input amplitude voltage. This is possible by adding common-mode voltage to the target output, as shown in Fig. 4, where this common-mode voltage consists of third harmonic of the input and output frequencies (ω_i and ω_o, respectively). Thus, the new output reference voltage (v'_{jref}) that allows the best use of the input voltage envelope is

$$v'_{jref}(t) = v_{jref}(t) + \frac{1}{4}V_i \cos(3\omega_i t) - \frac{1}{6}V_o \cos(3\omega_o t), \quad (1)$$

where V_i is the input voltage amplitude, V_o is the output voltage amplitude and v_{jref} is the output reference voltage ($j \in \{\text{a, b, c}\}$), of one phase as in (2). The input grid is considered ideal with input voltages (v_K, where $K \in \{\text{A, B, C}\}$) given by (3).

$$\begin{cases} v_{aref}(t) = V_o \cos(\omega_o t) \\ v_{bref}(t) = V_o \cos(\omega_o t + \frac{2\pi}{3}) \\ v_{cref}(t) = V_o \cos(\omega_o t + \frac{4\pi}{3}) \end{cases} \quad (2)$$

$$\begin{cases} v_A(t) = V_i \cos(\omega_i t) \\ v_B(t) = V_i \cos(\omega_i t + \frac{2\pi}{3}) \\ v_C(t) = V_i \cos(\omega_i t + \frac{4\pi}{3}) \end{cases} \quad (3)$$

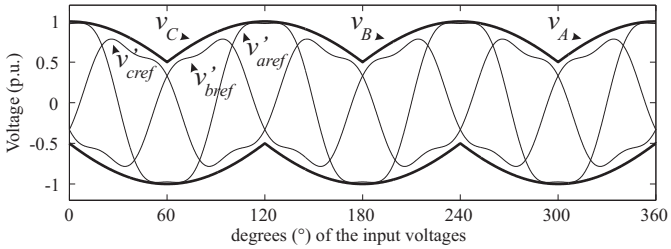

Fig. 4. Voltage ratio improvement to 87%.

The main features of the matrix converters are the following [2], [3], [5], [9], [10]:

- direct frequency conversion;
- simple and compact power circuit;
- none large energy storage element;
- output voltage with arbitrary amplitude and frequency;
- sinusoidal output voltage and input current waveforms;
- good input power factor for any load;
- bidirectionality (energy flux is allowed in both directions through the converter).

As disadvantages, it is possible to cite:

- complexity in the commutation and control schemes;
- intrinsical limit of the output voltage amplitude;
- difficulty in achieving Ride-Through capability.

Using matrix converter for adjustable speed drives leads to a compact drive solution. In this particular application, redesigning the motor to a lower nominal voltage is a valid solution to overcome the disadvantage of a lower voltage transfer ratio of matrix converter.

The purpose of this paper is to present two new scalar control strategies and their characteristics. The most popular scalar control techniques are used as references for comparison with the two new techniques. In the next section, a mathematical model, that is based in [5], is presented to give the necessary basis for explaining the operation principles of matrix converters.

II. MATHEMATICAL MODEL OF MATRIX CONVERTERS

The input and the output voltages can be expressed as vectors defined by:

$$\mathbf{v_i} = \begin{bmatrix} v_A(t) \\ v_B(t) \\ v_C(t) \end{bmatrix}, \quad \mathbf{v_o} = \begin{bmatrix} v_a(t) \\ v_b(t) \\ v_c(t) \end{bmatrix}. \quad (4)$$

where $\mathbf{v_i}$ and $\mathbf{v_o}$ are the input and the output voltage vectors, respectively. The input and the output voltages are related as:

$$\begin{bmatrix} v_a(t) \\ v_b(t) \\ v_c(t) \end{bmatrix} = \begin{bmatrix} S_{Aa}(t) & S_{Ba}(t) & S_{Ca}(t) \\ S_{Ab}(t) & S_{Bb}(t) & S_{Cb}(t) \\ S_{Ac}(t) & S_{Bc}(t) & S_{Cc}(t) \end{bmatrix} \begin{bmatrix} v_A(t) \\ v_B(t) \\ v_C(t) \end{bmatrix}, \tag{5}$$

or, in a simplified way using (4),

$$\mathbf{v_o} = \mathbf{S} \cdot \mathbf{v_i}, \tag{6}$$

where $\mathbf{S}$ is the instantaneous transfer matrix.

The switching function of a switch, S_{Kj} in Fig. 1, is defined as [11]:

$$S_{Kj} = \begin{cases} 1, & S_{Kj} \textit{ closed} \\ 0, & S_{Kj} \textit{ open} \end{cases}, \tag{7}$$

From Fig. 1, if two or more switches of the same output terminal are simultaneously closed, a short-circuit occurs in the input source. Another constraint that should be observed is related to the inductive nature of the load. If all the switches, in the same leg, are open simultaneously, an over-voltage occurs, which can damage the switches or any other device. These constraints can be expressed by:

$$S_{Aj}(t) + S_{Bj}(t) + S_{Cj}(t) = 1, \, \forall t. \tag{8}$$

In practice, it is difficult to respect the restriction (8). To avoid short-circuit in the input side of the converter and over-voltages in the output side, which can damage the bidirectional switches, some protection circuits must be employed. In the input side, the input filter may be used to minimize the short-circuit currents. The over-voltage problem can be solved using a diode clamp circuit ([5], [12] and [13]) or a varistor protection ([14]), depending of the power requested.

The input and the output currents, also defined by vectors, present the following relationship:

$$\begin{bmatrix} i_A(t) \\ i_B(t) \\ i_C(t) \end{bmatrix} = \begin{bmatrix} S_{Aa}(t) & S_{Ab}(t) & S_{Ac}(t) \\ S_{Ba}(t) & S_{Bb}(t) & S_{Bc}(t) \\ S_{Ca}(t) & S_{Cb}(t) & S_{Cc}(t) \end{bmatrix} \begin{bmatrix} i_a(t) \\ i_b(t) \\ i_c(t) \end{bmatrix}, \tag{9}$$

or

$$\mathbf{i_i} = \mathbf{S^T} \cdot \mathbf{i_o}, \tag{10}$$

where $\mathbf{i_i}$ and $\mathbf{i_o}$ are the input and the output current vectors, respectively, and $\mathbf{S^T}$ is the transpose of matrix $\mathbf{S}$.

The duty cycle in each switch determines the employed switching pattern. The difference among the several techniques used to synthesize the output voltages is strongly related to the duty cycles. The definition of the duty cycle (m_{Kj}) for the switch S_{Kj} is

$$m_{Kj}(t) = \frac{t_{Kj}}{T_s}, \tag{11}$$

where t_{Kj} is the time interval during which the switch S_{Kj} is closed in a switching period (T_s). Figure 5 shows a generic switching pattern for any output terminal j.

Considering that T_s is small enough, it is possible to suppose that $\mathbf{v_i}(t)$ is approximately constant during each interval T_s. Thus, the average value of the output voltage ($\overline{\mathbf{v}}_\mathbf{o}(t)$) is given by:

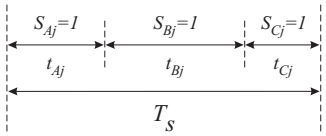

Fig. 5. Generic switching pattern for any output terminal j.

$$\overline{\mathbf{v}}_\mathbf{o}(t) = \mathbf{M}(t) \cdot \mathbf{v_i}(t). \tag{12}$$

Similarly, the relationship between input average current and output current (approximately constant during T_s) is

$$\bar{\mathbf{i}}_\mathbf{i}(t) = \mathbf{M}(t)^T \cdot \mathbf{i_o}(t), \tag{13}$$

where $\mathbf{M}(t)$ is defined as

$$\mathbf{M}(t) = \begin{bmatrix} m_{Aa}(t) & m_{Ba}(t) & m_{Ca}(t) \\ m_{Ab}(t) & m_{Bb}(t) & m_{Cb}(t) \\ m_{Ac}(t) & m_{Bc}(t) & m_{Cc}(t) \end{bmatrix}. \tag{14}$$

III. SCALAR PULSE WIDTH MODULATION TECHNIQUES

The scalar pulse width modulation (*PWM*) strategies presented here follow the chronological order of each technique publication. In the scalar modulation techniques, the switches duty cycles are determined from the input voltages instantaneous values by using simple algebraic equations. Thus, in these techniques voltage space vectors calculation is not necessary.[15].

A. Alesina and Venturini's Technique

In 1980, the first control strategy was proposed by *Venturini* [2]. This technique consists of composing a reference output voltage from the input voltages. To understand this process, a special vector notation is used, as shown in Fig. 6, at an instant t when $\mathbf{V_A}$ is aligned with the real axis.

The angle α presented in Fig. 6 is expressed by:

$$\alpha = (\omega_o - \omega_i)t, \tag{15}$$

which means the relative position between vectors $\mathbf{V_j}$ and $\mathbf{V_A}$.

The decomposition of $\mathbf{V_j}$ in the real and imaginary axes, in the complex plane, results in following equations:

$$V_{jX} = m_{Aj}V_A - m_{Bj}V_{BX} - m_{Cj}V_{CX}, \tag{16}$$

$$V_{jY} = m_{Bj}V_{BY} - m_{Cj}V_{CY}, \tag{17}$$

where X represents the vector components in the real axis and Y represents the vector components in the imaginary axis. The last equation necessary to calculate the duty cycles is given by (18), obtained from Fig. 5.

$$m_{Aj} + m_{Bj} + m_{Cj} = 1 \tag{18}$$

Solving (16), (17) and (18) results in:

$$m_{Kj} = \frac{1}{3}[1 + 2q\cos(\alpha - (h-1)\frac{2\pi}{3})], \tag{19}$$

where $h = 1$ for $K = A$, $h = 2$ for $K = B$, $h = 3$ for $K = C$ and q is the ratio between the amplitude of the output and the input voltages.

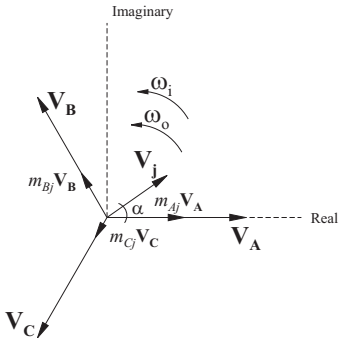

Fig. 6. Output voltage synthesis from the three input phase voltages.

These results for three-phase balanced output voltages are shown in Table I. This operation mode is known as symmetric mode.

TABLE I
Duty cycles in the symmetric and antisymmetric mode

K	j			K	j		
	a	b	c		a	b	c
A	h = 1	h = 3	h = 2	A	h'= 1	h'= 2	h'= 3
B	h = 2	h = 1	h = 3	B	h'= 2	h'= 3	h'= 1
C	h = 3	h = 2	h = 1	C	h'= 3	h'= 1	h'= 2

If the output reference voltage presents a rotating direction opposite to the direction analyzed before, another result for the duty cycles is obtained. This result is presented in (20).

$$m'_{Kj} = \frac{1}{3}[1 + 2q\cos(\alpha' - (h' - 1)\frac{2\pi}{3})], \qquad (20)$$

where the angle α' is

$$\alpha' = -(\omega_o + \omega_i)t, \qquad (21)$$

and the values of h' are shown in Table I. This operation mode is known as antisymmetric mode.

A general solution is obtained using (19) and (20):

$$\overline{\mathbf{v}}_\mathbf{o}(t) = [a\mathbf{M}(t) + b\mathbf{M}'(t)] \cdot \mathbf{v_i}(t), \qquad (22)$$

with $a + b = 1$. The change in the values of a and b affects, directly, the input displacement factor (*DF*) and to achieve unity input *DF* it is necessary to do $a = b = 0.5$.

Another way to reach the same results was proposed by *Venturini* and *Alesina* [3], in the same year. Knowing the output target voltages and the load, it is possible to know the output currents. As the input voltages are known and the instantaneous input power must be equal to the instantaneous output power, it is also possible to determine the input currents. The set of equations needed to reach the same result is composed by the condition given in (19) and knowing that the sum of the input currents must be equal to the sum of the output currents (Kirchhoff's currents law).

B. Rodríguez's Technique

This technique, proposed in 1983 [16], consists of a simple control strategy where the most positive and the most negative input voltages, called here v_P and v_N, respectively, are used to synthesize the output reference voltage. Assuming that the switching frequency (f_s) is much greater than the input and the output frequencies (f_i and f_o, respectively), it is considered that, during a switching period, the input and the output voltages are constant. Therefore, the author introduced the concept of fictitious bipolar source, which allows to control the converter in the same way as the well known *PWM* technique of the dc link inverters.

The used *PWM* was the classical sine-triangle modulation (basically an analog technique), which compares a high frequency triangular carrier (v_{tri}) with the reference signal, known as modulating signal, to create pulses for the switches of the power converter [15]. In a simple way, the technique operation is the following: if the triangular signal is greater than the reference output voltage (v_{jref}), the bidirectional switch connected to v_N is closed; otherwise, the bidirectional switch connected to v_P is closed.

C. Roy and April's Technique

Proposed in 1989, this technique [17] consists of generating the active and zero states of the bidirectional switches by using the instantaneous voltage ratio of specific input phase voltages, and comparing their relative magnitudes through the following rules:

Rule 1: At any instant, the input phase voltage which has different polarity from both others is assigned to V;

Rule 2: The two input phase voltages which have the same polarity are assigned to T and U, with the smallest voltage (in absolute value) being T.

Then t_T and t_U are chosen such that:

$$\frac{t_{Tj}}{t_{Uj}} = \frac{v_T}{v_U}, \qquad (23)$$

where t_{Tj} e t_{Uj} are the time intervals that the switches connected to v_T and v_U, respectively, are closed. To determine t_{Vj}, the time interval during which the switch connected to v_V is closed, (24) is used.

$$t_{Tj} + t_{Uj} + t_{Vj} = T_s, \qquad (24)$$

where the output reference voltage is given by

$$v_{jref} = \frac{1}{T_s}[t_{Tj}v_T + t_{Uj}v_U + t_{Vj}v_V] = V_o\cos(\omega_o t + \theta_o), \qquad (25)$$

where θ_o can be any phase angle value.

Using (23) and (24) in (25), for a balanced three phase system the following relationships can be obtained:

$$\frac{t_{Uj}}{T_s} = \frac{v_{jref} - v_V}{1.5V_i^2}v_U, \qquad (26)$$

$$\frac{t_{Tj}}{T_s} = \frac{v_{jref} - v_V}{1.5V_i^2}v_T, \qquad (27)$$

$$\frac{t_{Vj}}{T_s} = 1 - \frac{t_{Uj} + t_{Tj}}{T_s}. \qquad (28)$$

The average value of the input current is given by

$$\bar{i}_K = \frac{1}{T_s}[t_{Ka}i_a + t_{Kb}i_b + t_{Kc}i_c], \qquad (29)$$

where $K = \{A, B, C\}$. Substituting (26) or (27) or (28) with the different values of j ($j = \{a, b, c\}$) in (29), if $i_a + i_b + i_c = 0$, it is possible to reach

$$i_K = \frac{p_o}{1.5V_i^2} v_K, \tag{30}$$

where p_o is the total instantaneous power. Therefore, the output voltage v_j can be any kind of waveform, since that the output currents respect this constrain: $i_a + i_b + i_c = 0$.

This technique has also an interesting current phase displacement control, which consists of creating fictitious phase voltages at the matrix converter input terminal, as defined below

$$\begin{cases} v_A(t) = V_i \cos(\omega_i t + \psi) \\ v_B(t) = V_i \cos(\omega_i t + \psi + \frac{2\pi}{3}) \\ v_C(t) = V_i \cos(\omega_i t + \psi + \frac{4\pi}{3}) \end{cases} . \tag{31}$$

These fictitious voltages are employed to determine the duty cycles for each bidirectional switch by using the same rules. It follows that the input currents are in phase with their respective fictitious voltages and, consequently, they have a displacement angle of ψ related to the real input voltages. However, this procedure changes directly the amplitude of the output voltages through the following relation

$$V_o = qV_i \cos\psi. \tag{32}$$

For small values of ψ ($\psi < 15°$), this change is in the order of a few percent.

IV. THE TWO PROPOSED TECHNIQUES

In this section, two new and simple techniques are presented. In both, like the *Roy* and *April*'s technique, the instantaneous values of the input voltages are used to determine the duty cycles of the bidirectional switches. However, in these new techniques, just two input voltages are used in each switching period, reducing, so, the switching losses. In one of them, the most positive and the most negative input voltages, like the *Rodríguez*'s technique, are used to synthesize the desired output voltages. Even though, the duty cycles are calculated from the measured input voltages and the reference output voltages. The other technique uses the two input voltages which are nearest to the reference output voltage.

A. *Control Technique* 1

In this technique, the duty cycles are calculated from v_P and v_N (as defined in section III-B) and it is uses the fictitious dc link concept. Therefore, the obtained duty cycles are:

$$m_{Pj} = \frac{t_{Pj}}{T_s} = \frac{v_{jref} - v_N}{v_P - v_N}, \tag{33}$$

$$m_{Nj} = \frac{t_{Nj}}{T_s} = 1 - m_{Pj}, \tag{34}$$

where t_{Pj} and t_{Nj} are the time intervals in which the switches connected to the most positive and the most negative input voltages are closed, respectively.

The average value of the phase current, in each switching period (T_s), is given by:

$$\bar{i}_K = \frac{1}{T_s}[t_{Ka} i_a + t_{Kb} i_b + t_{Kc} i_c]. \tag{35}$$

In one period of the input voltages, each input voltage is, during a third of the period, equal to v_P, during another third, equal to v_N and, in the rest of the period (120○), equal to the input voltage that has the intermediate value (v_{int}). In the control strategy, v_{int} does not participate of the output voltages. Thus, in the input side, the three switches connected to v_{int} are opened and the current is equal to zero.

Using (33) in (35), it is possible to determine the current flowing in the most positive input terminal (i_P).

$$i_P = \frac{p_o}{v_P - v_N} \tag{36}$$

Similarly, to determine the current flowing in the most negative input terminal (i_n), (34) is used in (35).

$$i_N = \frac{p_o}{v_N - v_P} \tag{37}$$

Writing (36) and (37) in phasor notation:

$$I_P = I\angle -\gamma, \tag{38}$$

$$I_N = I\angle -\beta, \tag{39}$$

where I is equal to:

$$I = \frac{p_o}{\sqrt{3}V_i}, \tag{40}$$

γ is the phase angle of the voltage ($v_P - v_N$) and β is the phase angle of the voltage ($v_N - v_P$). $\beta = \gamma + 180$○, with the input voltage v_A phase angle as the reference. The use of the phasor notation is only applied to improve the understanding of the input currents behavior (it is easier to determine the envelope of the input currents).

Table II presents, by using (38) and (39), the envelope of the input currents (i_A, i_B, i_C) when the input voltages, corresponding to the same phase of the input current, are sequentially v_P, v_{int}, and v_N. Using Table II, it is possible to achieve the graphics, shown in Fig. 7, that relate the input phase currents with their input voltages.

TABLE II
Phasor behavior of the input phase currents

Input Voltages		Module ∠ Angle		
$\mathbf{v_P}$	$\mathbf{v_N}$	$\mathbf{i_A}$	$\mathbf{i_B}$	$\mathbf{i_C}$
v_A	v_B	$I\angle -30°$	$I\angle 150°$	0
v_C	v_B	0	$I\angle 90°$	$I\angle -90°$
v_C	v_A	$I\angle 30°$	0	$I\angle -150°$
v_B	v_A	$I\angle -30°$	$I\angle 150°$	0
v_B	v_C	0	$I\angle 90°$	$I\angle -90°$
v_A	v_C	$I\angle 30°$	0	$I\angle -150°$

Looking at Fig. 7, it is possible to verify that the fundamental input current is in phase with its input voltage and the *DF* is, naturally, equivalent to one. Thus, independently from the load connected to the output terminals of the matrix converter, the fundamental of the input currents are in phase with their input voltages.

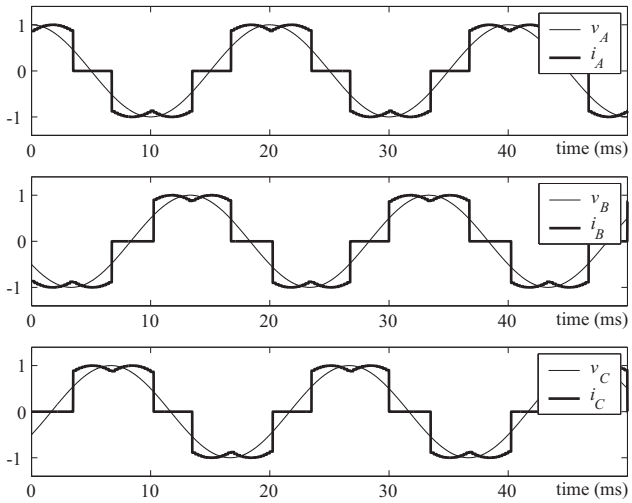

Fig. 7. Input phase voltages and input phase current envelopes (in p.u.).

B. Control Technique 2

This technique consists in determining which input voltages are nearest to the reference output voltage (v_{jref}), in each switching period. This can be done by determining which input voltage has the intermediate value (v_{int}) and, knowing v_{int}, the reference voltage is compared with v_{int}. If $v_{jref} > v_{int}$ the input voltages used to synthesize v_{jref} are v_P (the most positive input voltage) and v_{int}. If $v_{jref} < v_{int}$ the input voltages used to synthesize v_{jref} are v_N (the most negative input voltage) and v_{int}. Fig. 8 illustrates how this selection is achieved.

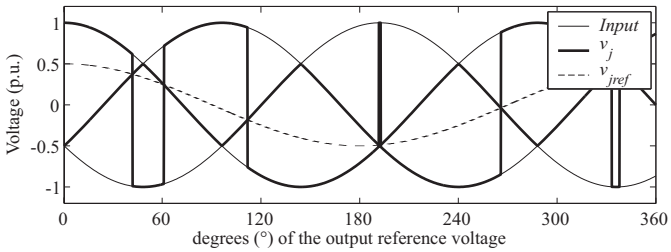

Fig. 8. Input phase voltages used to synthesize (in bold line) a reference output voltage (dashed line).

In average values, the desired output voltage is calculated from (41).

$$\overline{v}_{jref} = \frac{1}{T_s}[t_{majorj} v_{majorj} + t_{minorj} v_{minorj}] \qquad (41)$$

where v_{majorj} and v_{minorj} are determined as follow:

- $v_{jref} > v_{int} \Rightarrow \begin{cases} v_{majorj} = v_P \\ v_{minorj} = v_{int} \end{cases}$
- $v_{jref} < v_{int} \Rightarrow \begin{cases} v_{majorj} = v_{int} \\ v_{minorj} = v_N \end{cases}$

and t_{majorj} and t_{minorj} (the intervals during which the switches connected to the terminals corresponding to v_{major} and v_{minor}, respectively, are closed) are related as in (42).

$$t_{majorj} + t_{minorj} = T_s \qquad (42)$$

Then, it is necessary to have the duty cycles of the two bidirectional switches that are connected to the output terminals of the converter in each switching period. For this purpose, it is considered that, during T_s, the value of the input voltages as well as the value of the output voltages do not change (this approximation is valid for the same condition presented in section III-B - $f_i, f_o \ll f_s$). Therefore, using (42) in (41) results in (43) and (44).

$$m_{majorj} = \frac{t_{majorj}}{T_s} = \frac{v_{jref} - v_{minorj}}{v_{majorj} - v_{minorj}} \qquad (43)$$

$$m_{minorj} = \frac{t_{minorj}}{T_s} = 1 - m_{majorj} \qquad (44)$$

V. SIMULATION RESULTS

For comparing the different scalar techniques, some simulations (Fig. 9 - Fig. 13) have been done. For all techniques, the input grid is considered to be an ideal voltage source with the following characteristics:

- voltage amplitude (V_i): $100V$;
- frequency (f_i): $50Hz$.

For the output terminals of the matrix converter, it is desired a voltage amplitude (V_o) of $50V$ ($q = 0.5$, without common-mode voltage) and frequency (f_o) of $40Hz$ (any output frequency can be synthesized as long as the output and the input frequencies respect this restriction: $f_o, f_i \ll f_s$). The inductive load, with displacement factor of 0.866 ($\cos 30°$), has the following characteristics:

- inductance of $2mH$;
- resistance of 0.87Ω.

The bidirectional switches, in all cases, are considered to be ideals and the switching frequency (f_s) is $4kHz$ (in the *Rodríguez*'s technique the carrier frequency was also $4kHz$).

The simulation results were analyzed from the following variables:

- the output variables (figures (a) and (b)) and the frequency spectrum of the unfiltered line-to-line voltage (figures (e));
- the input variables (figures (c)) and the frequency spectrum of the unfiltered current (figures (f)) and the filtered input current (figures (d)).

Table III presents the Total Harmonic Distortion (THD) and Weighted THD (THD_w) for the input current (i_A), when a load with *DF* equals to 0.866 or 0.5 is connected to the converter output with the desired output voltage of $50V$. A filter can be connected to the converter input to minimize the voltage distortions and to eliminate the harmonic components of the input currents. For the filter design, the harmonic spectrum of the input currents must be analyzed. The *Alesina* and *Venturini*'s and *Roy* and *April*'s techniques present dominant harmonics only in switching frequency multiples. The other techniques present harmonic components near to the input frequency. In these simulations, the filter used was a 4^{th} order Butterworth filter with a cut-off frequency of $120Hz$.

Table IV presents the THD and THD_w for the output line voltage (v_{ab}) as well as the number of switchings for the control techniques in one switching period. In Table IV, different loads do not change the results. It can be seen that the *Alesina* and *Venturini*'s and *Roy* and *April*'s techniques have more switching losses than the other presented techniques.

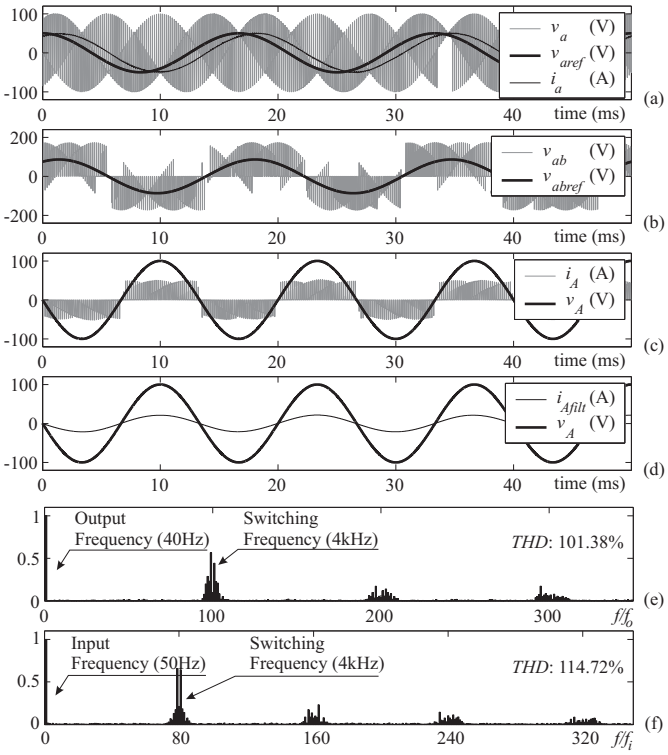

Fig. 9. Simulation results of the Alesina and Venturini's technique.

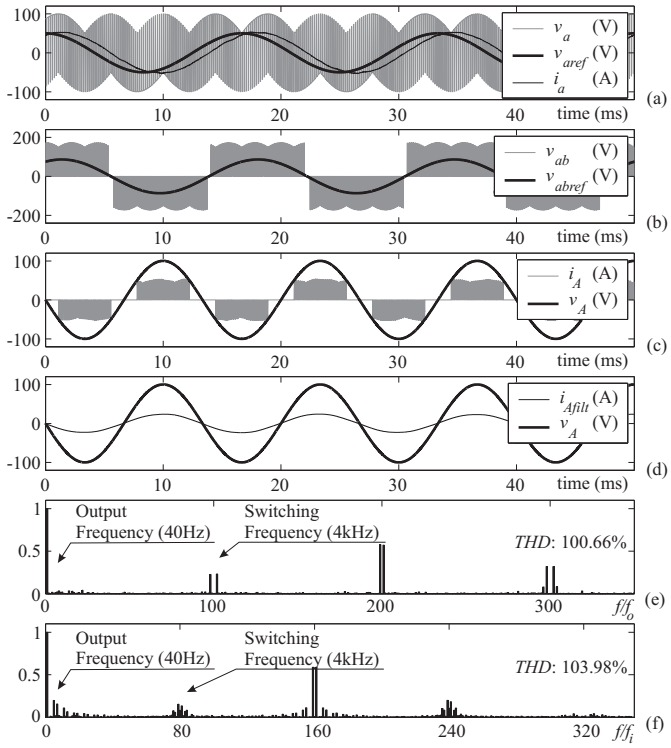

Fig. 10. Simulation results of the Rodríguez's technique.

TABLE III
Harmonic content for the input current

Control	DF=0.866		DF=0.5	
Technique	THD (%)	THD_w (%)	THD (%)	THD_w (%)
Venturini	114.72	1.62	151.88	2.97
Rodríguez	103.98	4.82	133.57	5.07
Roy	111.53	1.57	144.16	2.79
Technique 1	110.40	4.55	145.66	4.77
Technique 2	141.06	13.07	207.00	21.59

TABLE IV
Output voltage and number of switchings

Control	v_{ab}		Number of switchings
Technique	THD (%)	THD_w (%)	in a switching period
Venturini	101.38	1.02	9
Rodríguez	100.66	1.16	6
Roy	101.23	1.08	9
Technique 1	111.36	1.42	6
Technique 2	100.70	1.14	6

VI. CONCLUSION

In this paper, a review of the main scalar techniques for matrix converters has been explained with the purpose of presenting two different scalar techniques.

The simulation results show that all techniques reach the objective of synthesizing the output reference voltage. In the input terminals of the converter, it is observed that the first four techniques present an unity *DF* (Fig. 9 - Fig. 13, (c) and (d)). The input currents of *Alesina* and *Venturini*'s and *Roy* and *April*'s techniques are easily filtered because they present relevant harmonic values only near to the switching frequency and its multiples.

Despite the simplicity, the input current of the techniques using the most positive and the most negative input voltages to synthesize the reference output voltages present relevant low order harmonics because the intermediate input voltage is not used. As each input voltage has an intermediate value during one third of the period ($T_i = \frac{1}{f_i}$), then, its input current is zero during this interval (Fig. 10(c) and Fig. 12(c)).

About switching losses, the proposed techniques and the *Rodríguez*'s technique present only two input voltage changes during a switching period T_s (only two input voltages are used to synthesize the output voltages). Consequently, the losses related to the switching process are expected to be lower than the losses of the other techniques.

An important advantage of the control technique 2 is related to the output side of the converter. It is possible to "visualize" the fundamental of the output voltage, Fig. 13(a), which reaches the output line-to-line voltages with less harmonic components. On the other hand, the input currents present relevant harmonic components as much in low frequency as in high frequency.

Differently from the other techniques, it is not possible to determine the behavior of the input currents for the scalar control technique 2, because, depending of the desired frequency and amplitude of the output voltage, there are moments in which a specific input voltage does never participate of the output voltages synthesis (Fig. 13(c)), which produces zero permanence in the waveform of the input currents. The problem is that these zero permanence cannot be previously estimated for any desired output voltage. Therefore, it is not

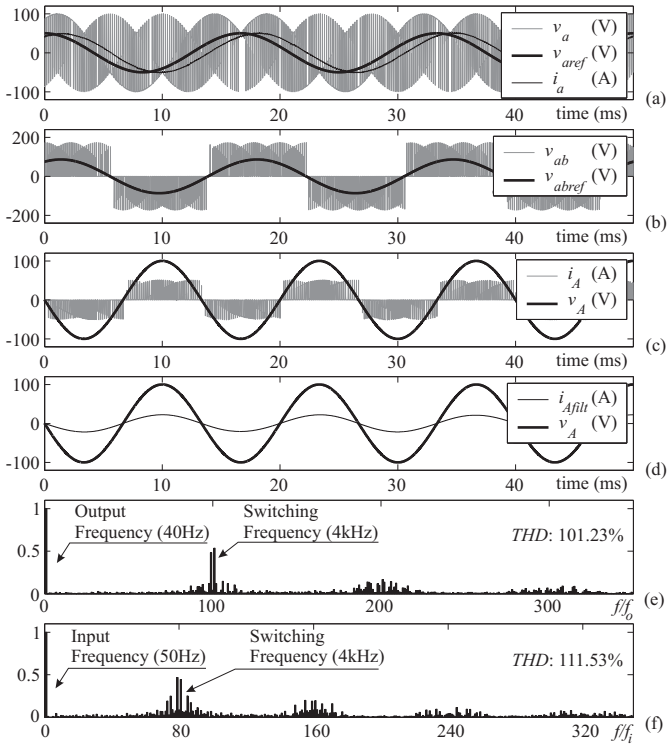

Fig. 11. Simulation results of the Roy and April's technique.

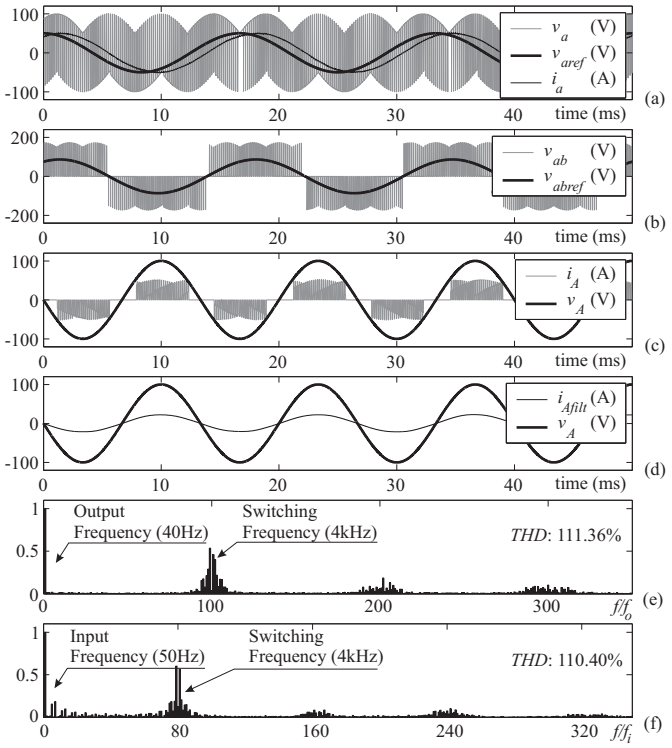

Fig. 12. Simulation results of the control technique 1.

possible to determine previously the input *DF*. In the other techniques, the *DF* can be controlled (the simulation results, from Fig. 9 to Fig. 11, present unity input *DF*). On the other hand, it is possible to observe that the behavior of the output voltage presents a better waveform quality.

Other simulations have been done to analyze the behavior of the input currents and output voltages with the addition of the common-mode voltage to the target output voltage, as shown in (1) and in Fig. 4. It has not been observed any changes related to the expected input currents and output line-to-line voltages and, therefore, a voltage ratio of 87% could be reached without any further problems.

REFERENCES

[1] L. Gyugyi and B. R. Pelly, *Static Power Frequency Changers: Theory, Performance, and Application*, John Wiley & Sons, 1976.

[2] M. Venturini, "A New Sine Wave In, Sine Wave Out Conversion Technique Eliminates Reactive Elements", in *Proc. POWERCON 7*, 1980, pp. E3_1 - E3_15.

[3] M. Venturini and A. Alesina, "The Generalized Transformer: A New Bidirectional Sinusoidal Waveform Frequency Converter With Continuously Adjustable Input Power Factor", in *Proc. IEEE PESC*, 1980, pp. 242 - 252.

[4] P. W. Wheeler, J. C. Clare, L. Empringham and M. Bland, "Matrix Converters: A Technology Review", *IEEE Trans. Ind. Electron.*, Vol. 49, Apr. 2002, pp. 276 - 288.

[5] P. W. Wheeler, J. Rodríguez, J. C. Clare, A. Weinstein, "Matrix Converters: A Technology Review", *IEEE Trans. Ind. Electron.*, Vol. 49, Apr. 2002, pp. 276 - 288.

[6] M. Hornonkamp, M. Loddenkötter, M. Münzer, O. Simon and M. Bruckmann, "EconoMAC the First All-in-One IGBT Module for Matrix Converters", in *Proceedings of Drives and Control Conference*, 2001, Internet.

[7] M. J. Maytum and D. Colman, "The Implementation and Future Potential of the Venturini Converter", in *IEEE Proc. Drives, Motors and Controls*, 1983, pp. 108 - 117.

[8] A. Alesina and M. Venturini, "Intrisic Amplitude Limits and Optimum Design of 9-Switches Direct PWM AC-AC Converters", in *Proc. IEEE PESC*, 1988, pp. 1284 - 1291.

[9] C. Klumpner, F. Blaabjerg, I. Boldea and P. Nielsen, "New Modulation Method for Matrix Converters", in *IEEE Transactions on Industry Applications*, vol. 42, n° 3, May-June 2006, pp. 797- 806.

[10] D. Casadei, F. Blaabjerg, I. Boldea and P. Nielsen, "A General Approach for the Analysis of the Input Power Quality in Matrix Converters", in *IEEE Transactions on Power Electronics*, vol. 13, n° 5, Sept. 1998, pp. 882- 891.

[11] L. Huber and D. Borojevic, "Space Vector Modulated Three-Phase to Three-Phase Matrix with Input Power Factor Correction", *IEEE Trans. Ind. Applicat.*, Vol. 31, Nov./Dec., 1995, pp. 1234 - 1246.

[12] C. Klumpner and F. Blaabjerg, "A New Matrix Converter-Motor (MCM) for Industry Applications", in *IEEE*, 2000, pp. 1394 - 1402.

[13] P. Nielsen, F. Blaabjerg and J. K. Pedersen, "New Protection Issues of a Matrix Converter: Design Considerations for Adjustable-Speed Drives", in *IEEE Transactions on Industry Applications*, Vol. 35, n° 5, September/October, 1999, pp. 1150 - 1161

[14] J. Mahlein and M. Braun, "A Matrix Converter without Diode Clamped Over-Voltage Protection", in *Proceedings of PIEMC'00*, 2000, pp. 817 - 822.

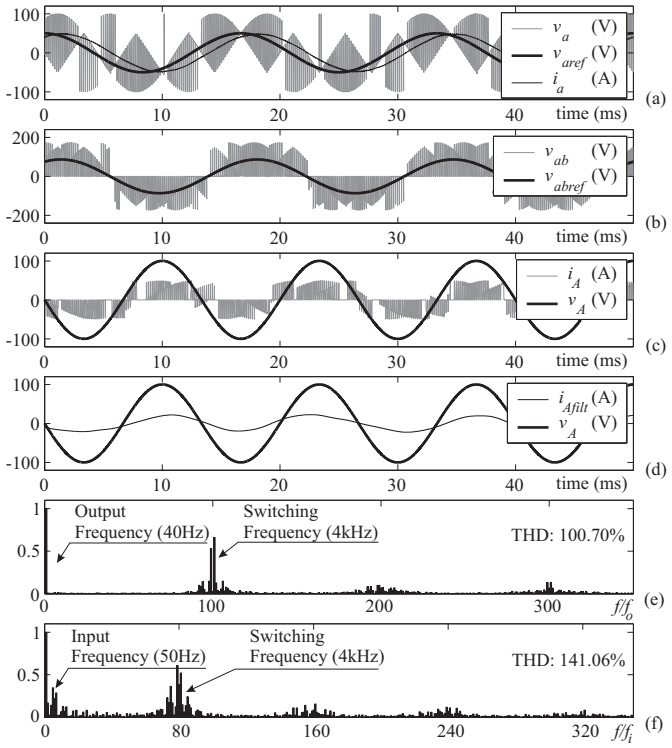

Fig. 13. Simulation results of the control technique 2.

[15] C. B. Jacobina, A. M. N. Lima, E. R. C. Silva, R. N. C. Alves, and P. F. Seixas, "Digital scalar pulse-width modulation: a simple approach to introduce non-sinusoidal modulating waveforms Power Electronics", in *IEEE Transactions on Power Electronics*, May 2001, pp. 351 - 359.

[16] J. Rodríguez, "A New Control Technique for AC-AC Converters", in *Proc. IFAC Control in Power Electronics and Electrical Drives*, 1983, pp. 203 - 208.

[17] G. Roy and G.-E. April, "Cycloconverter Operation Under a New Scalar Control Algorithm", in *Proc. IEEE PESC'89*, 1989, pp. 368 - 375.

BIOGRAPHIES

André G. H. Accioly was born in Recife, Brazil, in 1979. He received the B.S. and M.S. degrees in electrical engineering from the Federal University of Pernambuco, Recife, Brazil, in 2003 and 2006, respectively. His research interests are power electronics, frequency converters and power quality.

Vitor N. de Lima was born in Recife, Brazil, in 1983. He received the B.S. degree in electrical engineering in 2006 from the Federal University of Pernambuco, Recife, Brazil, where he is currently working toward the M.S. degree. His research interests are power electronics and power quality.

Fabrício Bradaschia was born in São Paulo, Brazil, in 1983. He received the B.S. degree in electrical engineering in 2006 from the Federal University of Pernambuco, Recife, Brazil, where he is currently working toward the M.S. degree. His research interests are power electronics and power quality.

Francisco A. S. Neves was born in Campina Grande, Brazil, in 1963. He received the B.S. and M.S. degrees in electrical engineering in from the Federal University of Pernambuco, Brazil, in 1984 and 1992, respectively, and the Ph.D. degree in electrical engineering in 1999 from the Federal University of Minas Gerais, Brazil. Since 1993, he has been at the Electrical Engineering and Power Systems Department, Federal University of Pernambuco, where he is currently a Professor of Electrical Engineering. His research interests are power electronics, renewable systems and power quality.

Marcelo C. Cavalcanti was born in Recife, Brazil, in 1972. He received the B.S. degree in electrical engineering in 1997 from the Federal University of Pernambuco, Recife, Brazil, and the M.S. and Ph.D. degrees in electrical engineering from the Federal University of Campina Grande, Campina Grande, Brazil, in 1999 and 2003, respectively. Since 2003, he has been at the Electrical Engineering and Power Systems Department, Federal University of Pernambuco, where he is currently a Professor of Electrical Engineering. His research interests are power electronics, renewable systems and power quality.

Antonio Samuel Neto was born in Recife, Brazil, in 1979. He received the B.S. and M.S. degrees in electrical engineering, in 2003 and 2005, respectively, from the Federal University of Pernambuco, Brazil, where he is currently working toward the Ph.D. degree in electrical engineering. His research interests are power electronics and renewable systems.